

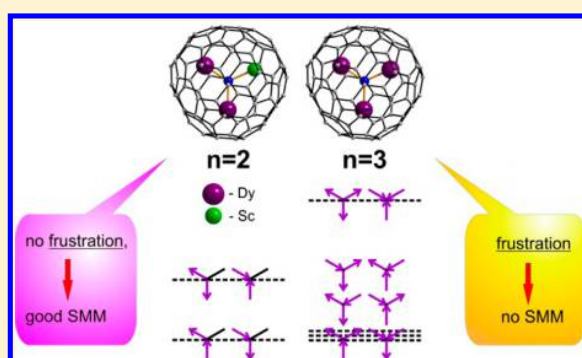
Key Role of Frustration in Suppression of Magnetization Blocking in Single-Molecule Magnets

Veacheslav Vieru, Liviu Ungur, and Liviu F. Chibotaru*

Theory of Nanomaterials Group, Department of Chemistry and Institute of Nanoscale Physics and Chemistry - INPAC, KU Leuven, Celestijnenlaan 200F, 3001 Leuven, Belgium

S Supporting Information

ABSTRACT: State-of-the-art ab initio calculations of a series of endohedral fullerenes $\text{Dy}_n\text{Sc}_{3-n}\text{N}@C_{80}$ ($n = 1, 2, 3$) are performed, and their anisotropic magnetic properties are described from the first principles. Contrary to general expectation that molecules of higher nuclearity (n) exhibit better magnetic blocking properties, we predict $\text{Dy}_3\text{N}@C_{80}$ to be a relatively weak single-molecule magnet due to its frustrated ground state. This finding, relevant to polynuclear magnetic molecules in general, demonstrates the crucial role played by magnetic frustration in the suppression of magnetization blocking in single-molecule magnets.



SECTION: Physical Processes in Nanomaterials and Nanostructures

Materials and devices involving anisotropic magnetic molecules have attracted recently much attention in view of several potential applications. These include magnetic memory at the scale of one molecule,^{1–3} molecular-scale spintronic devices,^{4–7} and qubits on the basis of magnetic molecules.^{8–11} A basic effect employed in these applications is the property of some anisotropic metal complexes to block the magnetic moment along the main anisotropy axis for a long period of time. Such complexes, called single-molecule magnets (SMMs),¹ behave pretty much as magnetic nanodomains or nanoparticles.¹² Efficient SMMs are characterized by long times of relaxation of magnetization, which is achieved in complexes with relatively high barriers for reversal of magnetization. The latter correspond to the energy of the excited magnetic state for which fast magnetization reversal occurs via quantum tunneling and/or spin–lattice relaxation. At the same time, lower-lying excited multiplets and the ground one are “opaque”, that is, they are characterized by much lower rates of reversal of magnetization. In the classical SMMs, like Mn_{12}ac and Fe_8 complexes,¹² the height of the barrier corresponds approximately to the zero-field splitting of the ground exchange multiplet. For metal ions with unquenched orbital momentum, the effect of blocking of magnetization can be achieved already in mononuclear complexes. Thus, mononuclear SMMs were first found on the example of lanthanide (Ln) complexes $[\text{LnPc}_2]^-$, Ln = Tb and Dy and Pc = dianion of phthalocyanine,¹³ and later also in actinide¹⁴ and first-row transition-metal complexes.¹⁵

The barrier of reversal of magnetization corresponds in this case to the energy of the first excited Kramers doublet (KD) on the metal site. Due to this capacity of individual Ln ions to

block (slow down) the reversal of magnetization, the magnetic relaxation in polynuclear Ln-based compounds, especially, in the mixed 4f–3d ones, is more complex than that in classical SMMs involving transition-metal ions only. For instance, it can display a coexistence of distinct single-ion and exchange-based blocking mechanisms.¹⁶

The single-ion blocking barrier in several Ln-based SMMs was found to be much higher than that in classical SMMs, on the order of several hundred wavenumbers,^{13,17} which sparked broad interest for their investigation.^{18,19} It was found, however, that mononuclear SMMs do not possess long relaxation times whatever the height of their barriers. The reason is the quantum tunneling of magnetization (QTM) in the ground doublet state of these complexes,^{20,21} which is usually much larger than that in polynuclear compounds. For this reason, the current strategy for the design of efficient SMMs is directed toward the synthesis of polynuclear complexes containing strongly anisotropic metal ions. The efficiency of this approach was recently demonstrated by the high SMM performance of binuclear complexes of Dy^{3+} ions coupled by the Ising exchange interaction²² and of Ln–radical bridged binuclear complexes.^{23,24} For the latter, the Dy–R–Dy complex has shown hysteresis of magnetization at a sweep rate of 0.08 T/s for temperatures up to 8.3 K,²³ while the Tb–R–Tb one is at a sweep rate of 0.9 mT/s for temperatures up to 14 K.²⁴ It is clear

Received: August 12, 2013

Accepted: October 3, 2013

Published: October 3, 2013

that judicious design of similar complexes of higher nuclearity can push their performances up.

Despite the importance of this research goal, there is no established strategy nowadays of building efficient SMMs from strongly anisotropic metal ions. The blocking properties of a series of isostructural polynuclear complexes can, for instance, demonstrate a counterintuitive trend of increase of relaxation time when one strongly anisotropic metal ion is replaced by a completely isotropic one.²⁵ Here, we concentrate on systems involving equivalent Ln ions with equal anisotropic properties and investigate theoretically how the blocking properties change with the increase of nuclearity of such complexes. An ideal object for our purposes is the series of dysprosium–scandium endofullerenes $\text{Dy}_n\text{Sc}_{3-n}\text{N}@C_{80}$, $n = 1-3$, for which a fully ab initio investigation of magnetic properties is undertaken. We find an unexpected result that the best SMM is obtained for $n = 2$, while the worst one is found for $n = 3$, which is explained by the magnetic frustration in the ground state of the latter compound. Thus, magnetic frustration is revealed to play a crucial role in the suppression of magnetization blocking in SMMs.

The structures of the investigated compounds $\text{Dy}_n\text{Sc}_{3-n}\text{N}@C_{80}$ are shown in Figure 1a–c. Each of them contains an

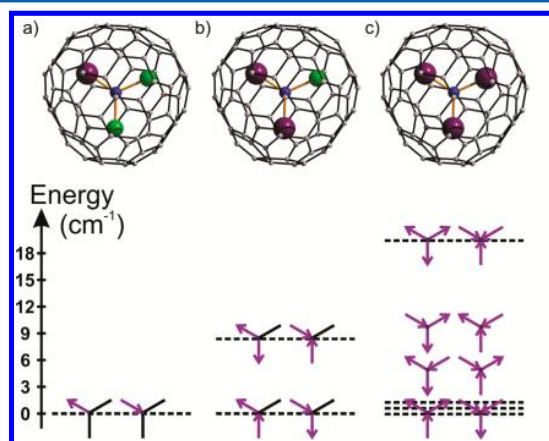


Figure 1. (a–c) Atomic structure of $\text{Dy}_n\text{Sc}_{3-n}\text{N}@C_{80}$ for $n = 1$ (a), 2 (b), and 3 (c). Legend for balls: large (indigo), Dy; second large (green), Sc; second small (blue), N; small (gray), C. (Lower panel) Low-lying energy levels (dashed lines) originating from the ground KD on Dy^{3+} (see Table 2). The magnetic structure of the corresponding Ising-like states is shown schematically by local magnetic moments on Dy^{3+} ions aligned along corresponding Dy–N bonds of the endohedral unit $\text{Dy}_n\text{Sc}_{3-n}\text{N}$. Time reversal components of each (exchange) doublet are shown on one horizontal level.

endohedral unit $\text{Dy}_n\text{Sc}_{3-n}\text{N}$ having geometry close to an equilateral triangle with the nitrogen atom in the center. Explicitly correlated (post Hartree–Fock) ab initio calculations of low-lying spin–orbital multiplets at individual Dy sites have been done within the complete active space self-consistent field approach (CASSCF)²⁶ by using the MOLCAS-7.8 package.²⁷ To this end, all Dy^{3+} ions except the investigated one have been replaced by the closed-shell Lu^{3+} ions without changing the coordinates of all other atoms of the $\text{Dy}_n\text{Sc}_{3-n}\text{N}@C_{80}$ molecule. The details of these calculations are described in the Supporting Information (SI), and the main results are given in Table 1. The results in the table correspond to DFT-optimized structures in the case of $n = 1$ ²⁸ and $n = 2$ (see the SI),

while for the complex with $n = 3$, the experimental structure has been used.²⁹ For the latter complex, the calculations for DFT-optimized structures show only insignificant deviations from the results in Table 1 (see the SI). The accuracy of the calculated multiplets and predictions based on them can be inferred from calculated field-dependent magnetization of the monodysprosium complex, showing very good agreement with experiment²⁸ (Figure S1, SI).

The ab initio calculations show that the ground KD at each Dy^{3+} center is strongly axial. This is evident from very small values of the obtained transversal g factors ($g_x g_y \approx 10^{-4}$ within the CASSCF approximation), for which a very small tunneling gap is expected. Thus, for a typical value of the internal field of $H_{\text{int}} = 20$ mT, we obtain $\Delta_{\text{tun}} = 1/2 g_x g_y \mu_B H_{\text{int}} \approx 10^{-6}$ cm⁻¹, which explains why $\text{DySc}_2\text{N}@C_{80}$ is a SMM.²⁸ Actually, the tunneling window in Dy^{3+} complexes is enlarged considerably by hyperfine coupling to nuclear spins,^{12,20} leading to significant QTM in the absence of a bias field, which is clearly seen from the waist-restricted magnetic hysteresis loops of this complex.²⁸ The evidence for strongly axial character of the crystal field at Dy sites comes from calculated g factors for the ground and first excited doublets along their main magnetic axes, which are close to pure $m_j = 15/2$ and $13/2$, respectively. However, as Table 1 shows, the main magnetic axes exhibit deviations from the corresponding Dy–N bonds. These deviations are larger for $\text{Dy}_2\text{ScN}@C_{80}$ because the Dy–N bonds in the Dy_2ScN triangle lack the two-fold rotational symmetry. The first excitation at Dy sites in all complexes lies significantly higher than that in most Dy complexes investigated so far, approaching the record values detected in terbium bisphthalocyanine sandwich complexes³⁰ and Dy_5 pyramids.¹⁷ The reason for that is the strong contribution of the nitrogen atom to the crystal field splitting of the atomic $J = 15/2$ multiplet on Dy sites of ~ 1500 cm⁻¹ on average (Table 1), which is 2–3 times larger than that in usual Dy complexes. To prove this, we carried out calculations for an isolated endohedral unit $[\text{DySc}_2\text{N}]^{6+}$ in its optimized geometry in the compound with $n = 1$. The results in Table 1 show that the crystal field splitting at Dy^{3+} is reduced by $\sim 30\%$ when the effect of the fullerene cage is removed. The contribution of the C_{80} cage to the axial component of the crystal field at dysprosium sites is expected to be similar. Table 1 also shows that the deviations of main magnetic axes at Dy sites from the corresponding Dy–N bonds are mainly due to the interaction with the fullerene cage. The latter is also responsible for significant reduction of the axiality of lowest KDs.

The magnetic properties of complexes with $n = 2$ and 3 are defined also by magnetic interactions between Dy1 and Dy2 and between Dy1–Dy2, Dy2–Dy3, and Dy1–Dy3 sites, respectively. These interactions include dipolar and exchange coupling of ground-state magnetic moments on neighboring sites. Given the strong axiality of ground KDs (Table 1), only the projection of the magnetic moment along the main magnetic axis Z_i (Figure 1b) at each Dy_i site, $\mu_{Z_i} = -(1/2)g_z \tilde{S}_{Z_i}$, will contribute to the dipolar interaction. Here, \tilde{S}_{Z_i} is the projection of pseudospin $\tilde{S}_i = 1/2$, describing the ground KD of the i th site,³¹ on the corresponding anisotropy axis. This means that the dipolar interaction between each pair of Dy sites is of noncollinear Ising form, $J_{\text{dip}}^{ij} \tilde{S}_{Z_i} \tilde{S}_{Z_j}$. On the other hand, the strong axiality on Dy centers, together with high energies of local excitations (Table 1), reduces the exchange interaction between lowest KDs on Dy centers to the same noncollinear Ising

Table 1. Energies of the Low-Lying KDs (cm^{-1}), g Tensors and Angles between the Main Anisotropy Axes and Dy–N Direction in $\text{Dy}_n\text{Sc}_{3-n}\text{N}@\text{C}_{80}$

KD	$\text{DySc}_2\text{N}^{6-}$		$\text{DySc}_2\text{N}@\text{C}_{80}$		$\text{Dy}_2\text{ScN}@\text{C}_{80}$		$\text{Dy}_3\text{N}@\text{C}_{80}$		
	Dy	Dy	Dy1	Dy2	Dy1	Dy2	Dy3	Dy3	Dy3
1	0	0	0	0	0	0	0	0	0
2	327	415	507	393	555	569	610		
3	594	747	812	777	852	879	923		
4	778	1002	1018	1074	1018	1083	1088		
5	864	1158	1161	1230	1145	1206	1221		
6	933	1256	1282	1303	1287	1332	1364		
7	1031	1334	1380	1382	1373	1458	1468		
8	1135	1465	1518	1514	1511	1533	1613		
g tensor of the ground and first excited KDs									
1	g_x	5.2×10^{-7}	8.3×10^{-5}	3.3×10^{-4}	8.3×10^{-5}	2.3×10^{-4}	1.4×10^{-4}	1.7×10^{-4}	
	g_y	6.4×10^{-7}	1.1×10^{-4}	4.3×10^{-4}	1.1×10^{-4}	3.3×10^{-4}	2.5×10^{-4}	2.4×10^{-4}	
	g_z	19.89	19.86	19.88	19.84	19.88	19.87	19.87	
2	g_x	1.4×10^{-4}	2.7×10^{-3}	1.8×10^{-2}	1.5×10^{-3}	2.4×10^{-2}	1.1×10^{-2}	1.4×10^{-2}	
	g_y	1.6×10^{-4}	2.9×10^{-3}	2.2×10^{-2}	1.7×10^{-3}	2.6×10^{-2}	1.2×10^{-2}	1.6×10^{-2}	
	g_z	17.05	17.10	17.03	17.03	16.96	17.04	16.90	
Angle between the main magnetic axis of the Kramers doublet g_z and the corresponding Dy–N axis (degrees)									
1	0.1	1.9	2.2	4.1	1.3	0.6	1.5		
2	0.1	7.4	5.8	0.5	2.5	8.4	1.3		

form.^{22,32} Then, the magnetic interaction between Dy ions is described by

$$\mathcal{H} = \sum_{\langle ij \rangle} (J_{\text{dip}}^{ij} + J_{\text{exch}}^{ij}) \tilde{S}_i \tilde{S}_j \quad (1)$$

where $\langle ij \rangle$ runs over pairs of Dy sites in the complex and the positive directions of Z_i and Z_j point outward from the central nitrogen atom.

With knowledge of the g tensor on Dy sites (Table 1), the constants of dipolar interaction are calculated straightforwardly (see Table 2). For the calculation of exchange-coupling constants, we used the Lines model,³³ which projects an effective isotropic exchange model $j_{ij} \mathbf{S}_i \cdot \mathbf{S}_j$ ($S_i = S_j = 5/2$ is the spin of the ground-state term on Dy^{3+}) into the anisotropic exchange interaction between the pseudospins $\tilde{S} = 1/2$ of the corresponding metal sites.^{22,32,34} If the latter is of noncollinear Ising type (eq 1), the corresponding exchange parameter is

Table 2. Magnetic Interactions and Low-Lying Exchange Spectrum Positions (cm^{-1}) in Didysprosium and Tridysprosium Complexes

interaction		$\text{Dy}_2\text{ScN}@\text{C}_{80}$	$\text{Dy}_3\text{N}@\text{C}_{80}$
J_{dip}	Dy1–Dy2	6.4	6.7
	Dy1–Dy3		6.8
	Dy2–Dy3		7.0
J_{exch}	Dy1–Dy2	10.8	12.2
	Dy1–Dy3		12.1
	Dy2–Dy3		14.0
exchange spectrum arising from the ground KDs on Dy ions		0.000000	0.000000
		0.000000	0.000000
		8.375903	0.033711
		8.375903	0.033711
			1.004686
			1.004686
			19.423231
			19.423231

expressed via the effective one as follows:³² $J_{\text{exch}}^{ij} = 25 \cos \varphi_{ij} j_{ij}$ where φ_{ij} is the angle between the anisotropy axes on the centers i and j . The effective exchange parameters have been estimated from broken-symmetry density functional theory (BS DFT) calculations (see the SI). To this end, we considered isostructural compounds in which Dy ions were replaced by Gd and derived the exchange parameters between the Gd ions. These exchange parameters were then rescaled from the spin 7/2 of Gd^{3+} to the spin 5/2 of Dy^{3+} and thus identified with the effective parameters j_{ij} of the Lines model. The validity of such scaling of effective exchange parameters is supported by a satisfactory description of magnetism in a series of Ln dimers³⁴ (see the SI). The resulting exchange parameters for different dysprosium pairs are shown in Table 2. One can notice relatively large values of J_{exch} as compared to other Dy complexes,^{22,34} which even exceed in the present case the usually dominant dipolar coupling. This is explained by a relatively strong Dy–N bond, which was also the reason for the large crystal field splitting on Dy sites.

The resulting spectrum positions of exchange states are given in Table 2, and their magnetic structures are given in the lower panel of Figure 1. Despite the fact that $\text{Dy}_2\text{ScN}@\text{C}_{80}$ is a non-Kramers complex, both of its exchange doublets appear to be degenerate at a high degree of accuracy. This is because the tunneling between the two magnetic configurations of the ground state (Figure 1) entrains simultaneous reversal of magnetic moments on both Dy centers, each of which is hardly achieved due to a very small transversal magnetic moment, as discussed above. For the same reason, the coupling between the two components of the ground exchange doublet via nuclear spins will be suppressed. Therefore, in contrast to the monodysprosium complex,²⁸ the hyperfine coupling is not expected to contribute efficiently to the opening of the tunneling window. Hence, the didysprosium complex is predicted to be a SMM with a long relaxation time and large magnetic remanence for temperatures significantly lower than the exchange splitting ($\sim 8 \text{ cm}^{-1}$; Table 2). Suppressed QTM in the ground exchange state means that activated relaxation

dynamics with the barrier corresponding to the first excited exchange state is expected for temperatures of several Kelvin. Therefore, two activated relaxation processes are expected in this complex, a high-temperature one related to relaxation via excited states on the individual Dy ions (the height of the barriers corresponds to the lowest excitations on Dy1 and Dy2; Table 1) and the low-temperature one related to surmounting the exchange barrier. The coexistence of two activation relaxation processes was observed in Co_2Dy_2 due to a relatively large Co–Dy exchange interaction,¹⁶ and here, it is expected to be detected due to the remarkably high Dy–Dy magnetic interaction.

In $\text{Dy}_3\text{N}@C_{80}$, the exchange splitting is roughly twice larger than that in the previous complex because each Dy has an Ising exchange interaction with two neighboring sites. The ferromagnetic dipolar and exchange coupling between Dy centers (Table 2) leads to the stabilization of three exchange KDs with the highest possible total magnetic moment ($\approx 20\mu_B$), approximately twice the moment of one Dy^{3+} . The corresponding magnetic configurations are shown in the lower panel of Figure 1. The relatively small splitting of these three low-lying exchange doublets, not exceeding 1 cm^{-1} , results mainly from slightly different values of the total magnetic interaction ($J_{\text{dip}} + J_{\text{exch}}$) obtained for the Dy2–Dy3 pair compared to the other two interacting pairs (Table 2). However, for magnetic measurements performed at usual temperatures (2–10 K), all three low-lying KDs are equally populated and therefore can be considered degenerate. The second factor underlying the obtained small splitting of the three exchange levels is the interaction of (almost) net Ising type between Dy sites. The quasidegeneracy of three exchange multiplets in the ground state gives rise to magnetic frustration in the complex, which is however quite different from the case of isotropic spins $1/2$ (for isotropic spins in the corners of an equilateral triangle, the ferromagnetic exchange interaction results in two degenerate exchange doublets in the ground state). Importantly, each magnetic configuration from the ground manifold is connected with other two by a single flip of the magnetic moment on one of the Dy sites (Figure 2). Hence, magnetic relaxation in each such configuration will be similar to that of the monodysprosium complex. Actually, the relaxation in $\text{Dy}_3\text{N}@C_{80}$ is expected to be faster than that in the latter complex due to the twice higher magnetic moment in the ground state, which is the source of the larger oscillating magnetic field in the paramagnetic phase of the crystal, causing ultimately higher QTM rates. We would like to emphasize that such behavior is entirely due to high quasidegeneracy of the ground state, which, in its turn, arises from frustration.

In summary, the ab initio investigation of three dysprosium–scandium–nitrogen-based endofullerenes $\text{Dy}_n\text{Sc}_{3-n}\text{N}@C_{80}$ predicts an irregular change of their magnetic blocking properties with the nuclearity n . Contrary to general expectations, the best SMM turns out to be not the tridysprosium complex but the didysprosium one. The latter has efficiently blocked QTM at low temperature because reversal of magnetization in its ground state requires simultaneous flip of magnetic moments on both Dy sites. On the contrary, $\text{Dy}_3\text{N}@C_{80}$ is expected to be the weakest SMM from the series because of its frustrated ground state allowing the QTM to proceed via reversal of the magnetic moment on one single Dy ion. Thus, magnetic frustration is revealed to play a crucial role in the suppression of magnetization blocking in SMMs. This finding has broad implications for the design of efficient polynuclear SMMs on

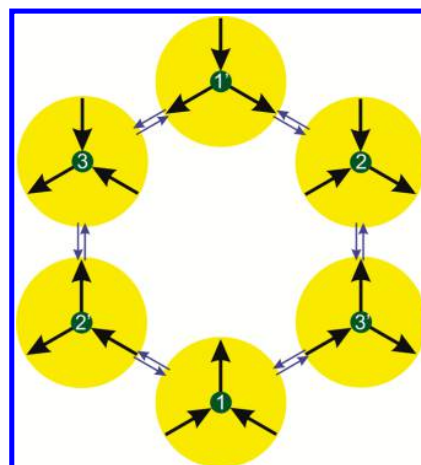


Figure 2. Scheme of connection of the lowest six magnetic eigenstates, corresponding to three low-lying quasidegenerate exchange levels of $\text{Dy}_3\text{N}@C_{80}$, $i = 1-3$ (Figure 1), via magnetic moment flip on one single Dy site. The i and i' are time-reversal components corresponding to one exchange KD (see Table 2). Black arrows represent the orientation of the magnetic moment of the corresponding Dy site.

the basis of strongly anisotropic metal ions. It implies, for instance, that even if one manages to avoid frustration in the ground state of such complexes, the frustration of excited states will most probably be a crucial limiting factor setting the height of the barrier significantly lower than the total exchange splitting.

■ ASSOCIATED CONTENT

■ Supporting Information

Details and results of (i) CASSCF calculations of the electronic structure of individual Dy sites, (ii) DFT calculations of parameters of exchange coupling between magnetic sites, (iii) calculation of the anisotropic exchange spectrum within the Lines model,³³ (iv) simulation of magnetism, and (v) Cartesian coordinates of all molecules. This material is available free of charge via the Internet at <http://pubs.acs.org>.

■ AUTHOR INFORMATION

■ Corresponding Author

*E-mail: Liviu.Chibotaru@chem.kuleuven.be.

■ Notes

The authors declare no competing financial interest.

■ ACKNOWLEDGMENTS

We would like to thank Thomas Greber and Rasmus Westerström for useful discussions and Alexey Popov for sending us DFT-optimized structures of investigated compounds. The project was supported by the Fonds Wetenschappelijk Onderzoek - Vlaanderen (FWO) and by GOA, INPAC, and Methusalem programs at the KU Leuven.

■ REFERENCES

- (1) Sessoli, R.; Gatteschi, D.; Caneschi, A.; Novak, M. A. Magnetic Bistability in a Metal-Ion Cluster. *Nature* **1993**, *365*, 141–143.
- (2) Christou, G.; Gatteschi, D.; Hendrickson, D. N.; Sessoli, R. Single-Molecule Magnets. *MRS Bull.* **2000**, *25*, 66–71.
- (3) Mannini, M.; Pineider, F.; Danieli, C.; Totti, F.; Sorace, L.; Sainctavit, Ph.; Arrio, M.-A.; Otero, E.; Joly, L.; Cezar, J. C.; et al.

Quantum Tunneling of the Magnetization in a Monolayer of Oriented Single-Molecule Magnets. *Nature* **2010**, *468*, 417–421.

- (4) Heersche, H. B.; de Groot, Z.; Folk, J. A.; van der Zant, H. S. J.; Romeike, C.; Wegewijs, M. R.; Zobbi, L.; Barreca, D.; Tondello, E.; Cornia, A. Electron Transport through Single Mn₁₂ Molecular Magnets. *Phys. Rev. Lett.* **2006**, *96*, 206801.
- (5) Loth, S.; von Bergmann, K.; Ternes, M.; Otte, A. F.; Lutz, C. P.; Heinrich, A. J. Controlling the State of Quantum Spins with Electric Currents. *Nat. Phys.* **2010**, *6*, 340–344.
- (6) Parks, J. J.; Champagne, A. R.; Costi, T. A.; Shum, W. W.; Pasupathy, A. N.; Neuscamman, E.; Flores-Torres, S.; Cornaglia, P. S.; Aligia, A. A.; Balseiro, C. A.; et al. Mechanical Control of Spin States in Spin-1 Molecules and the Underscreened Kondo Effect. *Science* **2010**, *328*, 1370–1373.
- (7) Bogani, L.; Wernsdorfer, W. Molecular Spintronics Using Single-Molecule Magnets. *Nat. Mater.* **2008**, *7*, 179–186.
- (8) Leuenberger, M. N.; Loss, D. Quantum Computing in Molecular Magnets. *Nature* **2001**, *410*, 789–793.
- (9) Lehmann, J.; Gaita-Arino, A.; Coronado, E.; Loss, D. Spin Qubits with Electrically Gated Polyoxometalate Molecules. *Nat. Nanotechnol.* **2007**, *2*, 312–317.
- (10) Timco, G. A.; Carretta, S.; Troiani, F.; Tuna, F.; Pritchard, R. J.; Murny, C. A.; McInnes, E. J. L.; Ghirri, A.; Candini, A.; Santini, P.; et al. Engineering the Coupling between Molecular Spin Qubits by Coordination Chemistry. *Nat. Nanotechnol.* **2009**, *4*, 173–178.
- (11) Luis, F.; Repolles, A.; Martinez-Perez, M. J.; Aguila, D.; Roubeau, O.; Zueco, D.; Alonso, P. J.; Evangelisti, M.; Camon, A.; Sese, J.; et al. Molecular Prototypes for Spin-Based CNOT and SWAP Quantum Gates. *Phys. Rev. Lett.* **2011**, *107*, 117203.
- (12) Gatteschi, D.; Sessoli, R.; Villain, J. *Molecular Nanomagnets*; Oxford University Press: Oxford, U.K., 2006.
- (13) Ishikawa, N.; Sugita, M.; Ishikawa, T.; Koshihara, S.; Kaizu, Y. Lanthanide Double-Decker Complexes Functioning as Magnets at the Single-Molecular Level. *J. Am. Chem. Soc.* **2003**, *125*, 8694–8695.
- (14) Rinehart, J. D.; Long, J. R. Slow Magnetic Relaxation in a Trigonal Prismatic Uranium(III) Complex. *J. Am. Chem. Soc.* **2009**, *131*, 12558–12559.
- (15) Freedman, D. E.; Harman, W. H.; Harris, T. D.; Long, G. J.; Chang, C. J.; Long, J. R. Slow Magnetic Relaxation in a High-Spin Iron(II) Complex. *J. Am. Chem. Soc.* **2010**, *132*, 1224–1225.
- (16) Mondal, K. C.; Sundt, A.; Lan, Y.; Kostakis, G. E.; Waldmann, O.; Ungur, L.; Chibotaru, L. F.; Anson, C. E.; Powell, A. K. Coexistence of Distinct Single-Ion and Exchange-Based Mechanisms for Blocking of Magnetization in a Co^{II}₂Dy^{III}₂ Single-Molecule Magnet. *Angew. Chem., Int. Ed.* **2012**, *51*, 7550–7554.
- (17) Blagg, R. J.; Murny, C. A.; McInnes, E. J. L.; Tuna, F.; Winpenny, R. E. P. Single Pyramid Magnets: Dy₅ Pyramids with Slow Magnetic Relaxation to 40 K. *Angew. Chem., Int. Ed.* **2011**, *50*, 6530–6533.
- (18) Sessoli, R.; Powell, A. K. Strategies Towards Single Molecule Magnets Based on Lanthanide Ions. *Coord. Chem. Rev.* **2009**, *253*, 2328–2341.
- (19) Woodruff, D. N.; Winpenny, R. E. P.; Layfield, R. A. Lanthanide Single-Molecule Magnets. *Chem. Rev.* **2013**, *113*, 5110–5148.
- (20) Ishikawa, N.; Sugita, M.; Wernsdorfer, W. Quantum Tunneling of Magnetization in Lanthanide Single-Molecule Magnets: Bis(phthalocyaninato)terbium and Bis(phthalocyaninato)dysprosium Anions. *Angew. Chem., Int. Ed.* **2005**, *44*, 2931–2935.
- (21) Meihaus, K. R.; Rinehart, J. D.; Long, J. R. Dilution-Induced Slow Magnetic Relaxation and Anomalous Hysteresis in Trigonal Prismatic Dysprosium(III) and Uranium(III) Complexes. *Inorg. Chem.* **2011**, *50*, 8484–8489.
- (22) Guo, Y.-N.; Xu, G. F.; Wernsdorfer, W.; Ungur, L.; Guo, Y.; Zhang, H. J.; Chibotaru, L. F.; Powell, A. K. Strong Axiality and Ising Exchange Interaction Suppress Zero-Field Tunneling of Magnetization of an Asymmetric Dy₂ Single-Molecule Magnet. *J. Am. Chem. Soc.* **2011**, *133*, 11948–11951.
- (23) Rinehart, J. D.; Fang, M.; Evans, W. J.; Long, J. R. Strong Exchange and Magnetic Blocking in N₂³⁻-Radical-Bridged Lanthanide Complexes. *Nat. Chem.* **2011**, *3*, 538–542.
- (24) Rinehart, J. D.; Fang, M.; Evans, W. J.; Long, J. R. A N₂³⁻ Radical-Bridged Terbium Complex Exhibiting Magnetic Hysteresis at 14 K. *J. Am. Chem. Soc.* **2011**, *133*, 14236–14242.
- (25) Ungur, L.; Thewissen, M.; Costes, J.-P.; Wernsdorfer, W.; Chibotaru, L. F. Interplay of Strongly Anisotropic Metal Ions in Magnetic Blocking of Complexes. *Inorg. Chem.* **2013**, *52*, 6328–6333.
- (26) Roos, B. O.; Taylor, P. R.; Siegbahn, P. E. M. A Complete Active Space SCF Method (CASSCF) Using a Density Matrix Formulated Super-CI Approach. *Chem. Phys.* **1980**, *48*, 157–173.
- (27) Aquilante, F.; De Vico, L.; Ferre, N.; Ghigo, G.; Malmqvist, P. A.; Neogady, P.; Pedersen, T. B.; Pitonak, M.; Reiher, M.; Roos, B. O.; et al. Software News and Update MOLCAS 7: The Next Generation. *J. Comput. Chem.* **2010**, *31*, 224–247.
- (28) Westerström, R.; Dreiser, J.; Piamonteze, C.; Muntwiler, M.; Weyeneth, S.; Brune, H.; Rusponi, S.; Nolting, F.; Popov, A.; Yang, S.; et al. An Endohedral Single-Molecule Magnet with Long Relaxation Times: DySc₂N@C₈₀. *J. Am. Chem. Soc.* **2012**, *134*, 9840–9843.
- (29) Yang, S.; Troyanov, S. I.; Popov, A.; Krause, M.; Dunsch, L. Deviation from the Planarity — A Large Dy₃N Cluster Encapsulated in an I_h-C₈₀ Cage: An X-ray Crystallographic and Vibrational Spectroscopic Study. *J. Am. Chem. Soc.* **2006**, *128*, 16733–16739.
- (30) Takamatsu, S.; Ishikawa, T.; Koshihara, S.-Y.; Ishikawa, N. Significant Increase of the Barrier Energy for Magnetization Reversal of a Single-4f-Ionic Single-Molecule Magnet by a Longitudinal Contraction of the Coordination Space. *Inorg. Chem.* **2007**, *46*, 7250–7252.
- (31) Chibotaru, L. F.; Ungur, L. *Ab Initio* Calculation of Anisotropic Magnetic Properties of Complexes. I. Unique Definition of Pseudospin Hamiltonians and their Derivation. *J. Chem. Phys.* **2012**, *137*, 064112.
- (32) Chibotaru, L. F.; Ungur, L.; Soncini, A. The Origin of Nonmagnetic Kramers Doublets in the Ground State of Dysprosium Triangles: Evidence for a Toroidal Magnetic Moment. *Angew. Chem., Int. Ed.* **2008**, *47*, 4126–4129.
- (33) Lines, M. E. Orbital Angular Momentum in the Theory of Paramagnetic Clusters. *J. Chem. Phys.* **1971**, *55*, 2977.
- (34) Long, J.; Habib, F.; Lin, P. H.; Korobkov, I.; Enright, G.; Ungur, L.; Wernsdorfer, W.; Chibotaru, L. F.; Murugesu, M. Single-Molecule Magnet Behavior for an Antiferromagnetically Superexchange-Coupled Dinuclear Dysprosium(III) Complex. *J. Am. Chem. Soc.* **2011**, *133*, 5319–5328.